Supplementary Information

Hollow Core-Shell Co_9S_8@In_2S_3 Nanotube Heterojunctions Toward Optimized Photothermal-Photocatalytic Performance

Ke Wang[a,1], Zhen Zhang[a,1], Tianzhi Cheng[a], Zipeng Xing[a,*], Zhenzi Li[b], Wei Zhou[a,b*]

[a] Department of Environmental Science, School of Chemistry and Materials Science, Key Laboratory of Functional Inorganic Material Chemistry, Ministry of Education of the People's Republic of China, Heilongjiang University, Harbin 150080, P. R. China,
Tel: +86-451-8660-8616, Fax: +86-451-8660-8240,
Email: xingzipeng@hlju.edu.cn; zwchem@hotmail.com

[b] Shandong Provincial Key Laboratory of Molecular Engineering, School of Chemistry and Chemical Engineering, Qilu University of Technology (Shandong Academy of Sciences), Jinan 250353, People's Republic of China

[1] K. Wang and Z. Zhang are contributed equally to this work.

Experimental section

Materials

Cobalt chloride hexahydrate ($CoCl_2 \cdot 6H_2O$, 99.99%), sodium sulfide (Na_2S, 95%) and indium trichloride tetrahydrate ($InCl_3 \cdot 4H_2O$, 99.99%) were purchased from Aladdin Reagent Company, China. Carbamide (CH_4N_2O, 99%), ethylene glycol (EG, 99.5%) and thioacetamide (TAA, 99%) were purchased from Sinopharm Chemical Reagent Co., Ltd. (Shanghai, China).

Characterization

X-ray diffractometer (XRD) patterns were collected on a Bruker D8 Advance diffractometer (using Cu Kα radiation, λ = 1.54056 Å, 40 kV, 40 mA). The morphology and structure of the products were characterized using field-emission scanning electron microscope (FE-SEM, Hitachi S-4800) and high-resolution transmission electron microscopy (HR-TEM, JEOL, JEM-2010). The chemical states of the elements on the surface of the samples were evaluated by the X-ray photoelectron spectrometer (XPS, PHI-5700 ESCA). All XPS data were corrected using the C 1s line at 284.6 eV, and curve fitting and background subtraction were accomplished. The light absorption ability was characterized by (UV-Vis) spectroscopy (UV3600, Shimadzu). N_2 adsorption/desorption was measured by a specific surface area analyzer (NOVA2000E). The samples were evacuated at 453 K for 24 h before analysis. Photoluminescence (PL) spectra were measured with a PE LS 55 spectrofluoro-photometer. Time resolved transient PL decay spectra of the prepared samples were obtained using a spectrophotometer (FLS1000, Edinburgh

Instruments, England). The water contact angles (CA) of the samples were determined by Contact angle meter (Dataphysics OCA 20, Germany).

DFT theoretical calculation

First-principle calculations were performed by the density functional theory (DFT) using the Vienna Ab-initio Simulation Package (VASP) package. The generalized gradient approximation (GGA) with the Perdew-Burke-Ernzerhof (PBE) functional were used to describe the electronic exchange and correlation effects. Uniform G-centered k-points meshes with a resolution of $2\pi*0.03$ $Å^{-1}$ and Methfessel-Paxton electronic smearing were adopted for the integration in the Brillouin zone for geometric optimization. The simulation was run with a cutoff energy of 500 eV throughout the computations. These settings ensure convergence of the total energies to within 1 meV per atom. Structure relaxation proceeded until all forces on atoms were less than 1 meV $Å^{-1}$ and the total stress tensor was within 0.01 GPa of the target value.

Photocatalytic hydrogen evolution

The photocatalytic H_2 evolution experiments were conducted in an online hydrogen generation system (Beijing Perfectlight, Labsolar-IIIAG). During the photocatalytic hydrogen evolution reaction, the samples (100 mg) were dispersed in 100 mL of methanol/H_2O solution ($V_{methaol}$:V_{H2O} = 1:4). Before light irradiation, the reactor and the entire gas circulating system were fully degassed to remove air using a vacuum pump for 30 min. A 300 W Xe lamp was used as the light source that simulated sunlight source. The photocatalytic H_2 evolution was analyzed using a gas

chromatograph (SP7800, TCD, molecular sieves 5 Å, N_2 carrier, Beijing Keruida Limited).

Apparent quantum efficiency (AQE)

The apparent quantum efficiency (AQE) was analyzed at 420 nm under the 300 W Xenon lamp (PLS-SXE300) irradiation. The other experimental conditions are similar to the photocatalytic hydrogen evolution measurement. The light intensity was obtained with an optical power meter (CEL-NP2000, CEAULIGHT, Beijing). For example, if 420 nm is used, the average light intensity is 18.65 mW cm^{-2}. The irradiation area is 28.3 cm^2 (3 cm radius). The number of incident photons is 1.61×10^{22} calculated by equation (1). The amount of H_2 molecules generated for 4 h were 1240.0 μmol. The AQE was then calculated in equation (2).

$$N = \frac{E\lambda}{hc} = \frac{18.65 \times 28.3 \times 10^{-3} \times 4 \times 3600 \times 420 \times 10^{-9}}{6.626 \times 10^{-34} \times 3 \times 10^{8}} = 1.61 \times 10^{22} \quad (1)$$

$$\begin{aligned} AQE &= \frac{\text{the number of reacted electrons}}{\text{the number of incident photons}} \times 100\% \\ &= \frac{2\times\text{the number of evolved } H_2 \text{ molecules}}{N} \times 100\% \\ &= \frac{2\times6.02\times10^{23}\times1240\times10^{-6}}{1.61\times10^{22}} \times 100\% = 9.3\% \end{aligned} \quad (2)$$

Photoelectrochemical tests

The electrochemical measurement was carried out by a standard three-electrode system. 50 mg as-prepared sample was dispersed in 35 mL ethanol and then spread uniformly on indium-tin oxide (ITO) conductor glass as work electrode, while Ag/AgCl as reference electrode, Pt foil as counter electrode and 1.0 M Na_2SO_4 aqueous solution as electrolyte. The transient photocurrent of the sample was obtained by multiple on/off light irradiation, with a period of 20 s. Electro-chemical impedance

spectroscopy was measured with amplitude of 5 mV and frequencies varying from 0.01 to 10000 Hz. Mott-Schottky was tested at a frequency of 2.5 kHz, and the whole experiment was conducted in the dark.

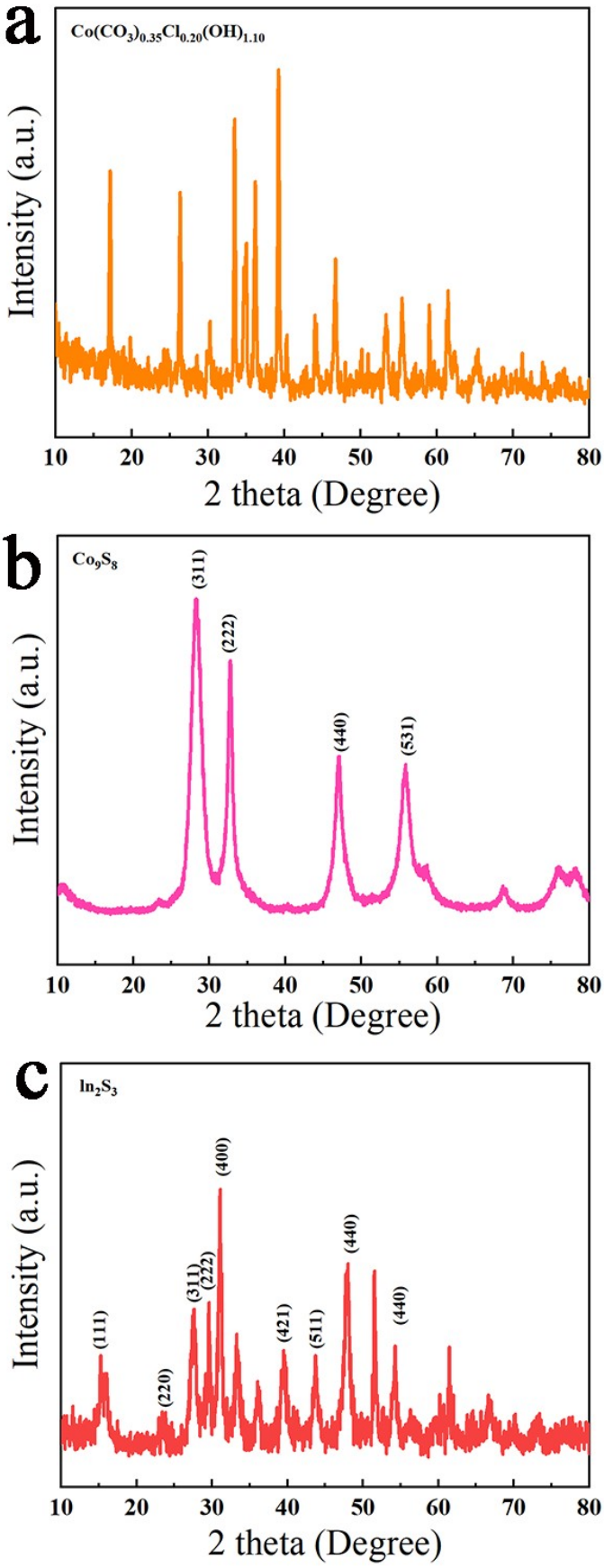

Fig. S1. XRD patterns of $Co(CO_3)_{0.35}Cl_{0.20}(OH)_{1.10}$ (a), Co_9S_8 (b) and In_2S_3 (c), respectively.

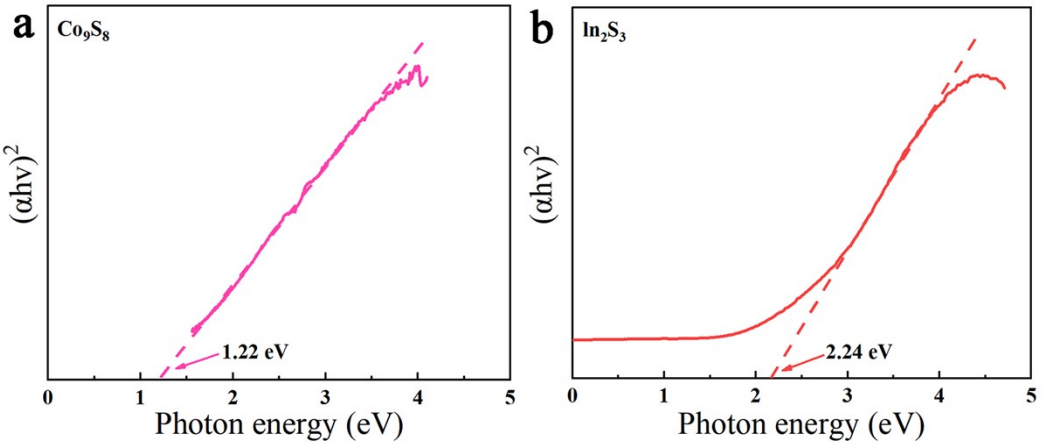

Fig. S2. The determination of indirect interband transition energies of Co_9S_8 (a) and In_2S_3 (b), respectively.

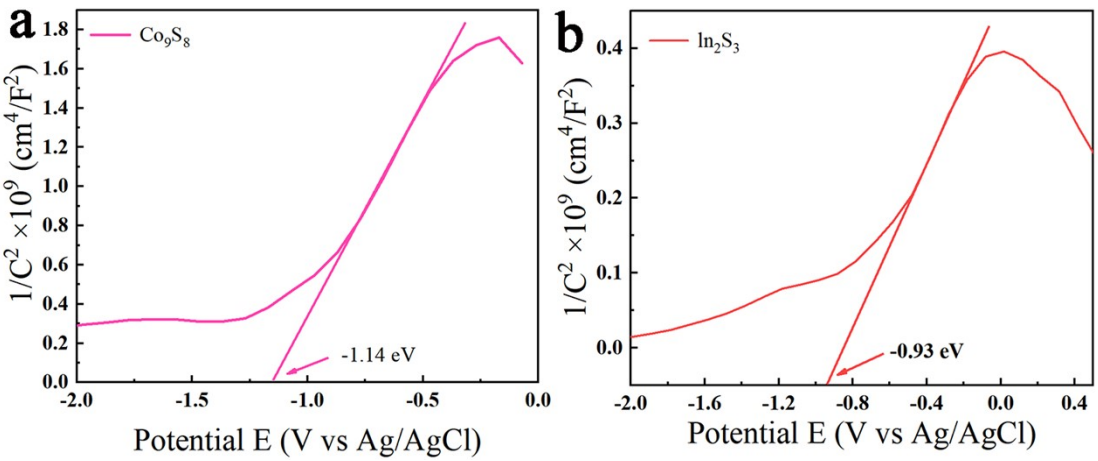

Fig. S3. Mott-Schottky plots of Co_9S_8 (a) and In_2S_3 (b) in Na_2SO_4 solutions, respectively.

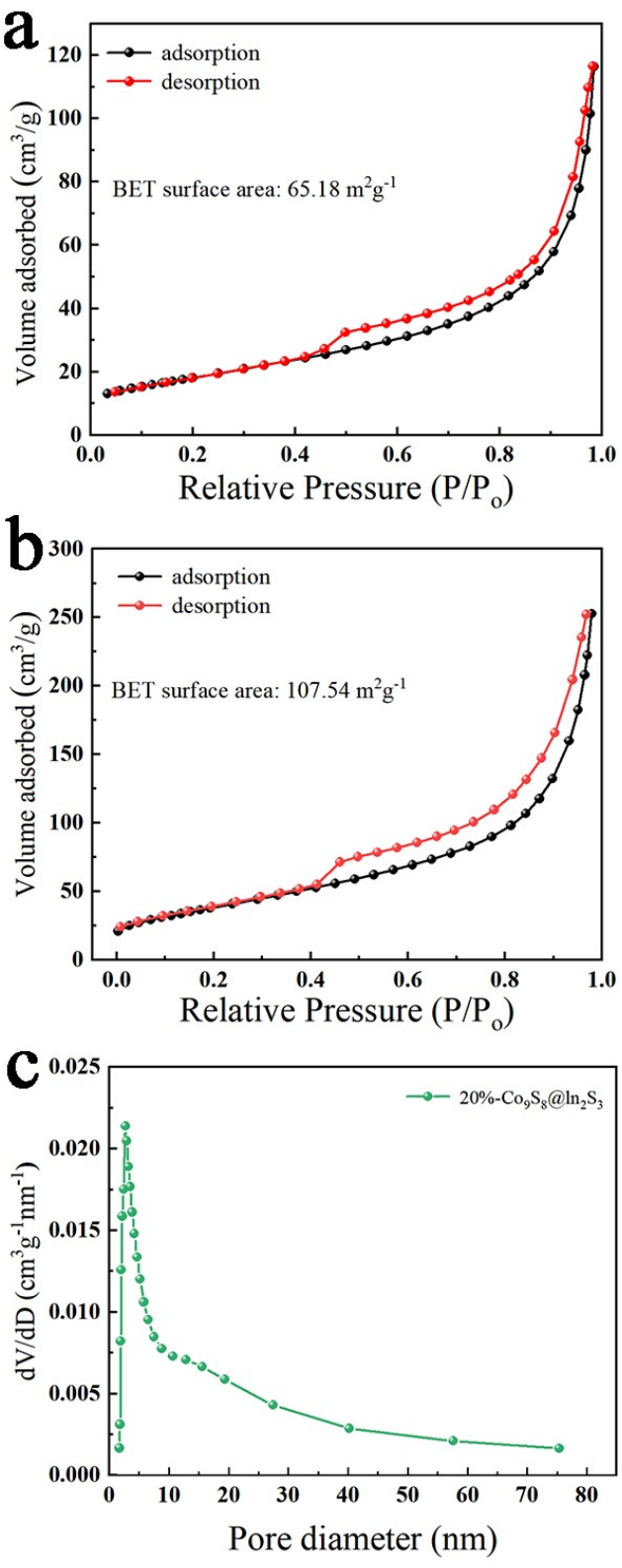

Fig. S4. N_2 adsorption-desorption isotherms of Co_9S_8 (a) and 20%Co_9S_8@In_2S_3(b), and the corresponding pore size distributions of 20%Co_9S_8@In_2S_3.

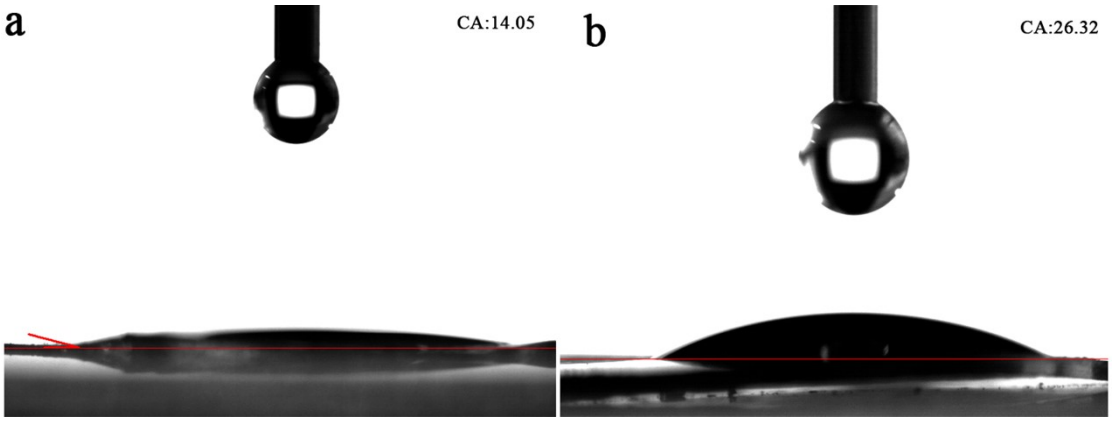

Fig. S5. The water contact angles of Co_9S_8 (a) and 20%Co_9S_8@In_2S_3, respectively.

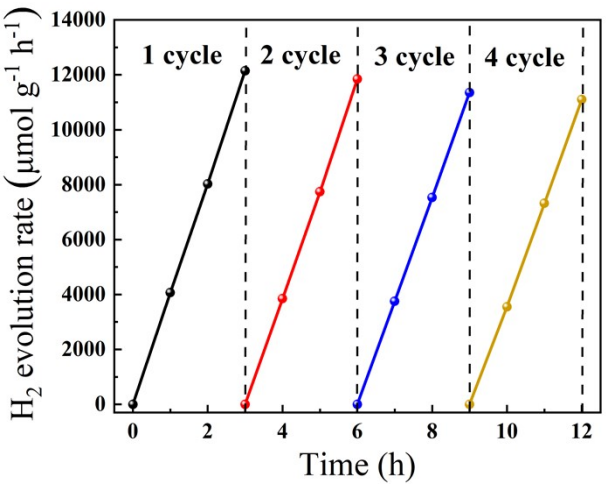

Fig. S6. Recycle tests of 20%Co_9S_8@In_2S_3 for photocatalytic H_2 evolution.

Table S1. The photocatalytic hydrogen rate of different In_2S_3-based photocatalysts.

Photocatalysts	Rate of H_2 generatio0n ($\mu mol \cdot g^{-1} \cdot h^{-1}$)	ref
In_2S_3-WC-MoS_2	136.76	[1]
GO/Fe_2P/In_2S_3	390.52	[2]
In_2S_3/In_2O_3	485.92	[3]
Mo_2C-In_2S_3	535.58	[4]
In_2S_3-TiO_2	614.2	[5]
In_2S_3-$Ni_{0.2}Mo_{0.8}N$(Ni)	637.9	[6]
In_2S_3/$CdIn_2S_4$/In_2O_3	2004	[7]
This Work	**4072.0**	

References

[1] M. Liu, P. Li, S. Wang, Y. Liu, J. Zhang, L. Chen, J. Wang, Y. Liu, Q. Shen, P. Qu, H. Sun, *J. Colloid Interface Sci.*, 2021, **587**, 876-882.

[2] X. Ma, W. Li, C. Ren, H. Li, X. Liu, X. Li, T. Wang, M. Dong, S. Liu, S. Chen, *J. Alloy. Comd.*, 2021, **875**, 160058.

[3] X. Li, X. Lyu, X. Zhao, Y. Zhang, S.N. Akanyange, J.C. Crittenden, H. Zhao, T. Jiang, *Int. J. Hydrogen Energy*, 2021, **46**, 18376-18390.

[4] X. Ma, C. Ren, H. Li, X. Liu, X. Li, K. Han, W. Li, Y. Zhan, A. Khan, Z. Chang, C. Sun, H. Zhou, *J. Colloid Interface Sci.*, 2021, **582**, 488-495.

[5] C. Wang, W. Qi, Y. Zhou, W. Kuang, T. Azhagan, T. Thomas, C. Jiang, S. Liu, M. Yang, *Chem. Eng. J.*, 2020, 381, 122611.

[6] Q. Hu, G. Chen, Y. Wang, J. Jin, M. Hao, J. Li, X. Huang, J. Jiang, *Nanoscale*, 2020, 12, 12336-12345.

[7] D. Ma, J.-W. Shi, Y. Zou, Z. Fan, J. Shi, L. Cheng, D. Sun, Z. Wang, C. Niu, *Nanoscale*, 2018,

10, 7860-7870.